OPEN ACCESS Freely available online

PLOS ONE

# Chimaerin Suppresses Rac1 Activation at the Apical Membrane to Maintain the Cyst Structure

**Shunsuke Yagi[1], Michiyuki Matsuda[1,2], Etsuko Kiyokawa[2,3]***

**1** Laboratory of Bioimaging and Cell Signaling, Graduate School of Biostudies, Kyoto University, Yoshida Konoe-cho, Sakyo-ku, Kyoto, Japan, **2** Department of Pathology and Biology of Diseases, Graduate School of Medicine, Kyoto University, Yoshida Konoe-cho, Sakyo-ku, Kyoto, Japan, **3** Department of Oncologic Pathology, Kanazawa Medical University, Uchinada, Kahoku-gun, Ishikawa, Japan

## Abstract

Epithelial organs are made of a well-polarized monolayer of epithelial cells, and their morphology is maintained strictly for their proper functions. Previously, we showed that Rac1 activation is suppressed at the apical membrane in the mature organoid, and that such spatially biased Rac1 activity is required for the polarity maintenance. Here we identify Chimaerin, a GTPase activating protein for Rac1, as a suppressor of Rac1 activity at the apical membrane. Depletion of Chimaerin causes over-activation of Rac1 at the apical membrane in the presence of hepatocyte growth factor (HGF), followed by luminal cell accumulation. Importantly, Chimaerin depletion did not inhibit extension formation at the basal membrane. These observations suggest that Chimaerin functions as the apical-specific Rac1 GAP to maintain epithelial morphology.

**Citation:** Yagi S, Matsuda M, Kiyokawa E (2012) Chimaerin Suppresses Rac1 Activation at the Apical Membrane to Maintain the Cyst Structure. PLoS ONE 7(12): e52258. doi:10.1371/journal.pone.0052258

**Editor:** Ed Manser, Astar-Neuroscience Research Partnership (NRP) and Institute of Medical Biology (IMB), Singapore

**Received** August 15, 2012; **Accepted** November 9, 2012; **Published** December 20, 2012



**Funding:** This work was supported by grants from the Ministry of Education, Culture, Sports, Science, and Technology of Japan. S. Yagi was supported by research fellowships from the Japan Society for the Promotion of Science for Young Scientists.The funders had no role in study design, data collection and analysis, decision to publish, or preparation of the manuscript.

**Competing Interests:** The authors have declared that no competing interests exist.

* E-mail: kiyokawa@kanazawa-med.ac.jp

## Introduction

Epithelial organs, such as kidney, mammary gland, salivary gland, and pancreas, contain cysts and tubules, which are both lumen-enclosing structures, although tubules are cylindrical instead of spherical [1]. Observing these structures in the living animal is technically challenging. Recently, three-dimensional cell culture in gels of extracellular matrix (ECM) allowed a close approximation of the biological situation *in vitro*. Madin Darby canine kidney (MDCK) cells form cysts consisting of a monolayer of polarized cells surrounding a lumen in Matrigel gels; therefore, they have been used to investigate molecular mechanisms for polarity and morphology [1].

By applying Raichu Förster Resonance Energy Transfer (FRET) biosensors to the MDCK cyst system, we recently visualized Rac1 activation during cystogenesis [2]. Rac1 activation was uniform in the entire plasma membrane of MDCK cysts in immature cysts, whereas in mature cysts, the activity became lower at the apical membrane than the lateral membrane. We also set up the system to induce activation or inactivation of the small GTPase Rac1 in different stages of polarity maturation, and found that the forced activation of Rac1 at the apical membrane disrupted apico-basal polarity to reorient cell division axes into the luminal space. In these cysts, cells accumulated in the lumen, which resembles hyperplasia *in vivo*. In contrast, suppression of Rac1 at the basolateral plasma membrane did not significantly affect the morphology of mature cysts. Therefore, it is now established that Rac1 suppression at the apical membrane is required for the mature cyst to maintain its morphology. What remained to be solved is which molecules suppress Rac1 activity at the apical membrane.

Rac1 belongs to the Rho family of small GTPases, which work as intracellular molecular switches and activate their downstream signaling molecules upon perception of external or internal cues [3]. GTP-bound, but not GDP-bound, small GTPases are able to bind to and activate effector proteins. Cycling between GDP- and GTP-bound states is controlled primarily by two classes of regulatory molecules: GTPase-activating proteins (GAPs), which enhance the relatively slow intrinsic GTPase activity of small GTPases; and guanine nucleotide-exchange factors (GEFs), which catalyze the exchange of GDP for GTP *in vivo*. Various GEFs and GAPs have been identified for Rho family GTPases, and their targets overlap [4;5], [6]. Since GAPs for Rho family GTPases share a conserved domain, it is not possible at this moment to predict their substrates by their amino-acid sequences [7]. Moreover, discrepancies have been reported between *in vitro* and *in vivo* specificities [6]. Therefore, to identify the GEF responsible for morphology, RNA interference (RNAi) screening was utilized [8], [9]. This method, however, requires enormous work to cover all of the GAPs for Rac1.

In this work, comparing messenger RNA levels between early and late stages of cystogenesis, we first identified which GAPs for Rho family GTPases become expressed in the late stages. Focusing on the lipid distribution assessed by FRET biosensors, we narrowed the list of candidates down to Chimaerin as a suppressor of Rac1 activity at the apical membrane. Chimaerin localized to the apical membrane, probably by diacylglycerol binding, and depletion of Chimaerin caused Rac1 activation there, followed by luminal cell accumulation in the presence of hepatocyte growth factor. These data indicate that Chimaerin is the specific GAP that

suppresses Rac1 activation at the apical membrane to maintain the cyst structure.

## Methods

### Plasmids

Plasmids for FRET biosensors Raichu-Rac1 have been reported previously [2]. CFP of from the original FRET biosensor for DIGDA and Pippi [10–12] was replaced with TFP, and cloned into the pCX4neo retroviral vector. Mouse β2-chimaerin cDNA was amplified from pEF-BOS-HA-2-chimaerin (a gift from Dr. Hironori Katoh, Kyoto University), and cloned into a pCX4bsr-EGFP plasmid. For shRNA-mediated knockdown experiments, shRNA sequences were: gattatgtccggttatgta (shLuc), ggtgtgaatactgtgctaact (shChn1), and gctggaagagtgattaataaa (shChn2). Corresponding DNA oligomers were cloned into pSUPER vector (Oligoengine, Seattle, WA).

### Cyst Culture

MDCK cells were purchased from RIKEN BioResource Center (No. RCB0995), and maintained in minimal essential medium (MEM) containing Earle's balanced salt solution (GIBCO) supplemented with 10% fetal bovine serum (Equitech-Bio), 3% L-Gln, 0.1% non-essential amino acids, 1 mM sodium pyruvate, 100 units/ml penicillin, and 100 μg/ml streptomycin, in a 5% $CO_2$ humidified incubator at 37°C.

### Retroviral Gene Transfer

To establish the MDCK cells stably expressing FRET biosensors, GFP-β2-chimaerin, dKeima, and shRNAs, in their respective retroviral expression vectors were packaged in BOSC23 cells co-transfected with the packaging plasmid pGP and the envelope plasmid pCMV-VSV-G-Rsv-Rev (provided by Hiroyuki Miyoshi and Atsushi Miyawaki, RIKEN). After infection of MDCK cells with the respective viral stocks, the cells were subjected to selection for 2 days with 2 mg/ml of G418 for pCX4neo vectors, 2 μg/ml of puromycin for pCX4puro vectors, and 10 μg/ml of blasticidin for pCX4bsr vectors.

### HGF Stimulation

Conditioned medium containing HGF produced by MRC-5 cells has described previously [2]. In this study, 1X conditioned medium was used for HGF stimulation.

### Microarray Analysis

To prepare cysts in early and late stages, MDCK cells were cultured with Matrigel for 2 and 10 days. Cysts in Matrigel were incubated with 1.25 mM EDTA/phosphate buffered saline (PBS) on ice for 1 hour to depolymerize the Matrigel, followed by washing three times with PBS. The cysts were centrifuged and stored in liquid nitrogen. RNA purification and microarray experiments [Canine (V2) Gene Expression Microarray (Agilent Technologies)] and analysis [Agilent Feature Extraction] were performed by Takara Bio Inc (Shiga, Japan).

### Quantitative PCR

Total RNA was purified with an RNeasy Micro Kit (QIAGEN, Hilden, Germany) and was reverse-transcribed using a High Capacity cDNA Reverse Transcription kit (Applied Biosystems, Foster City, CA) according to the manufacturer's protocol. mRNA Expression of Chn1, Chn2, and GAPDH mRNAs was analyzed by Power SYBR Green PCR Master Mix (Applied Biosystems) with an ABI PRISM7300 Sequence Detection System (Applied Biosystems). Primers used for quantitative PCR were: Chn1 forward, gccgcgttgaacgatatac; Chn1 reverse, tcttcgtttttgataagcagctc; Chn2 forward, gccactctactccgagaaaaag; Chn2 reverse, cgcttgtttttcttgattcattt; GAPDH forward, tccctcaagattgtcagcaa; and GAPDH reverse, tggatgactttggctagagga.

### Confocal Microscopy

Details of imaging and image acquisition settings were described in a previous report [2]. Briefly, cysts on Matrigel were placed on glass-bottom dishes containing $CO_2$-independent medium (GIBCO) containing 2% Matrigel, and imaged with an IX81 inverted microscope (Olympus) or BX upright microscope equipped with an FV1000 confocal imaging system (Olympus).

For imaging HGF-induced structures (Figure 1A), samples were examined on a BX upright microscope (Olympus) equipped with an FV1000 confocal imaging system (Olympus) and XLUMPLFL 20X W/0.98. The excitation laser and fluorescence filter settings were as follows: excitation laser for CFP/FRET, 440 nm; excitation dichroic mirror, DM405–440/515; CFP channel PMT dichroic mirror, SDM 510; CFP channel PMT filter, BA465–495; FRET channel PMT dichroic mirror; FRET channel PMT filter, BA520–550 nm.

For imaging cysts (Figure 2A, B, C, D, and Figure 3D), an IX81 inverted microscope (Olympus) equipped with an FV1000 confocal imaging system (Olympus), UPlanSApo 60X O/1.35 was used. The excitation laser and fluorescence filter settings were as follows: excitation laser, 440 nm; excitation dichroic mirror, DM405–440/515; CFP channel PMT dichroic mirror, SDM 510; CFP channel PMT spectral setting, 460–500 nm; FRET channel PMT dichroic mirror; FRET channel PMT spectral setting, 515–615 nm.

### Image Analysis

All fluorescence images and FRET images were processed with MetaMorph software (Universal Imaging, West Chester, PA) and calculated with Excel software (Microsoft) as described previously [2].

### Image Processing for Chn2 Localization

Before imaging, cysts were treated with 0.01% of saponin for 1 minute and fixed with 0.25% PFA/PBS for 30 minutes. After background subtraction from the fluorescence intensity of GFP and Keima, a GFP (500 multiplication)/Keima ratio image was processed and expressed using pseudocolor mode (MetaMorph).

### Statistical Analysis

All statistical analysis used Student's paired t-test in GraphPad prism software (La Jolla, CA).

## Results and Discussion

### Rac1 Activation Upon Hepatocyte Growth Factor Stimulation

The aim of this study is to understand the role and the mechanism underlying the polarized Rac1 activity in epithelial cells. For this purpose, we employed MDCK cells expressing Raichu-Rac1, a FRET biosensor of Rac1. In Matrigel, MDCK cells grow to form cysts, wherein Rac1 activity is suppressed at the apical plasma membrane. After the maturation of the cysts, MDCK cells were stimulated with Hepatocyte Growth Factor

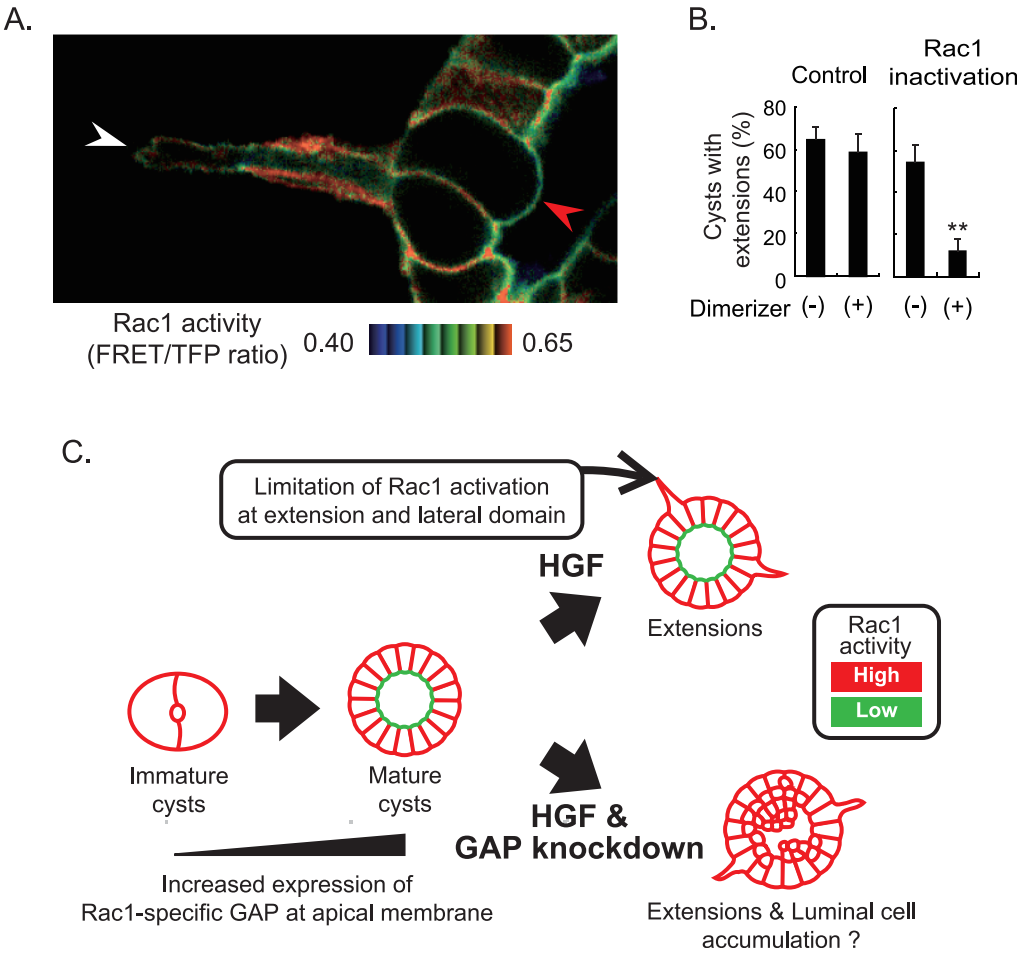


**Figure 1. Spatio-temporal regulation of Rac1 activity.** (A) MDCK cells expressing Raichu-Rac1 were cultured to form cysts for 10 days, treated with HGF for 12 hours, and imaged with an upright confocal microscope. White and red arrowheads indicate an extension and the apical membrane, respectively. The calculated FRET efficiency was colored in intensity-modulated display (IMD) modes as shown at the bottom. The upper and lower limits of the ratio range are shown at the bottom. (B) MDCK cysts expressing Lyn-FRB alone (Control) or with FKBP fused to the GAP domain of β2-chimaerin (Rac1 inactivation) were treated with HGF and Dimerizer for 12 hours (Supplemental Fig. S1). Shown are the averages of three independent experiments with standard deviation (SD). The numbers of scored cysts are: Experiment (Exp.) 1 [n = 53 (control, Dimerizer (−)), 76 (control, Dimerizer (+)), 100 (Rac1 inactivation, Dimerizer (−)), 88 (Rac1 inactivation, Dimerizer (+))]; Exp. 2 [n = 104, 106, 79, 70]; Exp. 3 [67, 97, 101, 84]. **P<0.01. (C) Schematic view of the concept of this study (see the main text).
doi:10.1371/journal.pone.0052258.g001

(HGF), which drives MDCK cells initially to extend the basal membrane outward and later to form tubular structures [13]. In HGF-stimulated MDCK cells, Rac1 activity was high at the baso-lateral plasma membrane, including the extended basal membrane, and low at the apical plasma membrane (Fig. 1A, white arrow head). To examine the role of Rac1 in the HGF-induced tubular extension, we utilized a rapamycin-mediated Rac1 inhibition system (Fig. S1) [2]. In this system, rapamycin, called dimerizer hereafter, is used to induce hetero-dimer formation between fragments of mammalian target of rapamycin (FRB) and FK506-binding protein (FKBP). In MDCK cells expressing both FRB tagged with myristylation signal of Lyn (Lyn-FRB) and FKBP fused with the GAP domain of β2-chimaerin (FKBP-GAP), the dimerizer translocates GAP to the plasma membrane and thereby inactivates Rac1. The MDCK cells were first cultured for 12 hours to form cysts and then stimulated with HGF in the presence or absence of the dimerizer. In the control cyst, which expressed only Lyn-FRB, approximately 60% of the cysts showed extensions irrespective of the presence of the dimerizer (Figure 1B, left graph). In the MDCK cells expressing both Lyn-FRB and FKBP-GAP, 55% of the cysts exhibited tubular extension in the absence of the dimerizer, but only 12% did so in the presence of dimerizer (Figure 1B, right graph). This result indicated that Rac1 is required for the HGF-mediated extension formation.

Importantly, Rac1 activity at the apical membrane remained low in the HGF-stimulated MDCK cells (Fig. 1A, red arrow head). Previously, we showed that forced Rac1 activation at the apical membrane causes luminal cell filling [2]. In contrast to this finding, HGF did not induce luminal cell filling. To explain this difference, we speculated that the presence of a Rac1 GAP at the plasma membrane enforces low Rac1 activity even in the presence of HGF (Fig. 1B). The Rac1 GAP would satisfy two criteria: first, the expression increases during cyst maturation; second, the Rac1 GAP is localized at the apical plasma membrane of the cells.

## Screening for Molecules to Regulate Rac1 Activity during Cystogenesis

We searched for the Rac1-specific GAP that fulfilled the aforementioned expression criterion by mRNA microarray

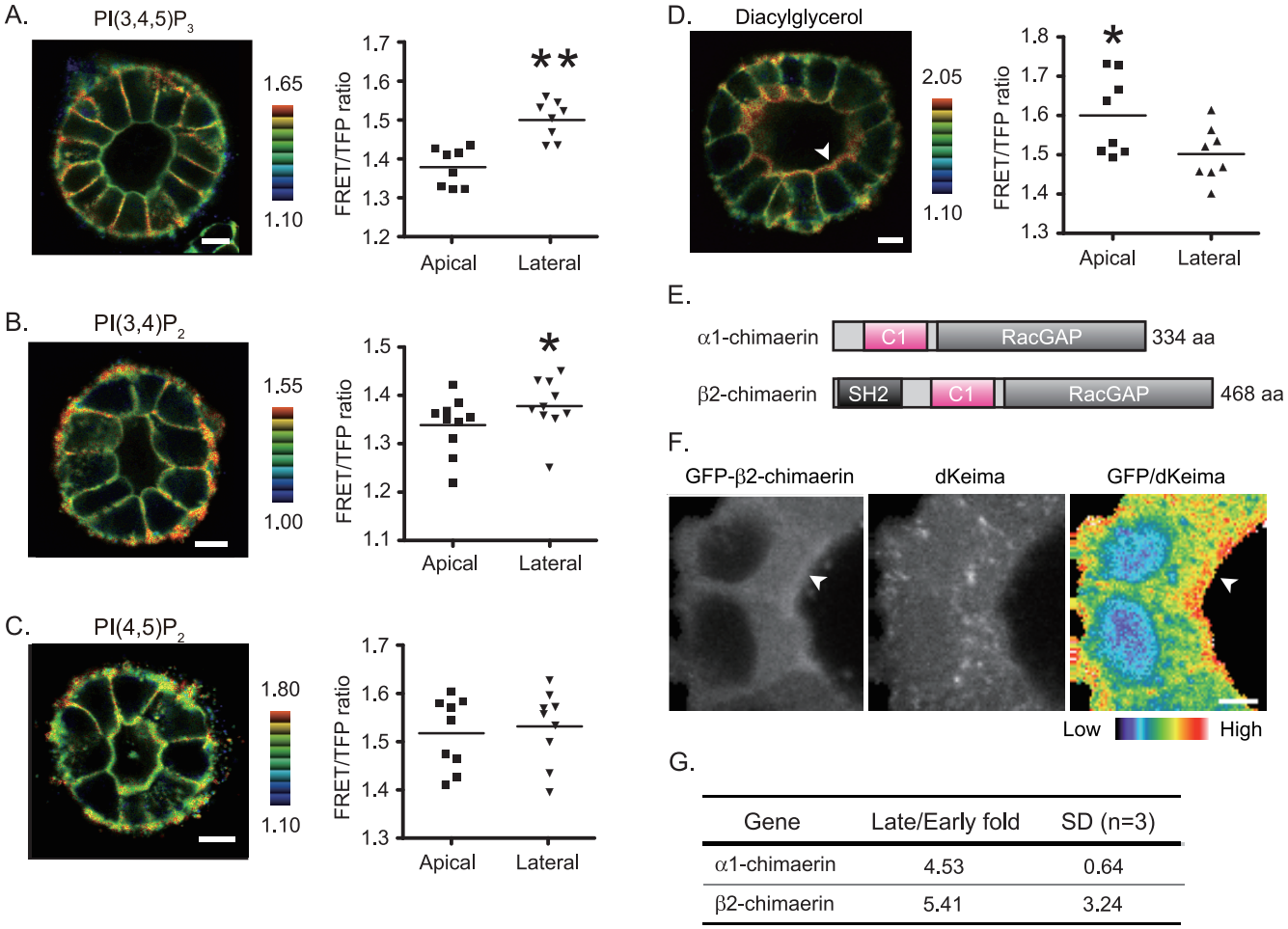


G.

| Gene | Late/Early fold | SD (n=3) |
|---|---|---|
| α1-chimaerin | 4.53 | 0.64 |
| β2-chimaerin | 5.41 | 3.24 |

**Figure 2. Localization of lipids and Chn2 in cysts.** FRET images and quantitative analysis of $PI(3,4,5)P_3$ (A), $PI(3,4)P_2$ (B), $PI(4,5)P_2$ (C) and diacylglycerol (D). The calculated FRET efficiency was colored and shown as in Fig. 1A.The white arrowhead in (D) indicates accumulation of diacylglycerol at the apical membrane. * $P<0.05$ and ** $P<0.01$ (E) Schematic view of α1- and β2-Chimaerin encoding 334 and 468 amino acids (AA). SH2 denotes the Src Homology 2 domain. (F) MDCK cysts expressing both dKeima and GFP-β2-Chimaerin were processed and imaged as described in Methods. Localization of GFP-β2-Chimaerin shown in GFP channel (left), dKeima channel (middle) and relative localization of GFP-β2-chimaerin over dKeima (right) shown in pseudocolor mode (at the bottom). White arrowheads indicate apical enrichment of GFP-β2-chimaerin. Scale Bar = 5 μm. (G) Results of quantitative PCR from cysts in early (2 days) and late (10 days) stages. Shown are the averages from three independent experiments with SD.
doi:10.1371/journal.pone.0052258.g002

analysis. MDCK cells were cultured in the Matrigel for 2 or 10 days before extraction of mRNAs, which were subjected to mRNA microarray analysis. In mammalian cells, there are about 30 proteins that are predicted to possess GAP activity against Rac1 [6]. Thirty-three GAPs for Rho-family GTPases were present in the microarray analysis used in this study (Supplemental Table S1). Seven genes were enriched more than 2-fold in cells isolated from late stages (Table 1).

## Enrichment of Diacylglycerol at the Apical Membrane and Identification of Chimaerins as Diacylglycerol-binding GAPs

Localization of GAPs is often regulated by inositol phosphates or diacylglycerol (DAG) [6]. To filter the candidate GAPs further by the second criterion, i.e. apical localization, we examined whether or not each GAP binds to these lipids. Before this, we needed to determine which phospholipids or DAG were enriched at the plasma membrane. We previously developed FRET biosensors for these lipids (Figure S1) [11;14;15]. To use retroviral-mediated gene transfer, the cyan emitting fluorescent protein in these biosensors was replaced by teal fluorescence protein as previously described [2]. We found that phosphatidylinositol (3,4,5) trisphosphate ($PIP_3$) and phosphatidylinositol (3,4) bisphosphate [$PI(3,4)P_2$] were enriched at the lateral membrane. These observations are consistent with ours [16], and others with a GFP-tagged PH domain [17]. Although the report with a GFP-tagged PH domain showed that $PI(4,5)P_2$ is enriched at the apical plasma membrane [17], $PI(4,5)P_2$ was found evenly distributed at the entire plasma membrane with the FRET-based biosensor (Fig. 2C). In striking contrast to the phospholipids, DAG preferentially accumulated at the apical membrane (Fig. 2D). Quantitative analysis confirmed the significant bias in the localization of $PI(3,4)P_2$, $PIP_3$, and DAG between the apical and lateral plasma membranes. Among them, only DAG was enriched at the apical plasma membrane (Figure 2A, B, C, D, right graphs). These observations prompted us to search for GAPs with a DAG binding domain such as a cysteine-rich motif, C1 domain. Among six candidate GAPs in Table 1, a C1 domain was found only in N-Chimaerin and β-Chimaerin [18].

**Table 1.** GAPs showing changes in mRNA levels between the early and late stages.

| Gene Name | Also known as | Log2 | Specificity * | Lipid binding domain ** |
|---|---|---|---|---|
| ARHGAP24 | FilGAP | 2.91 | Rac1, Cdc42 [32] | PH |
| CHN1 | | 2.17 | Rac1 [33] | C1 domain [19] |
| CHN2 | | 1.36 | Rac1 [34] | C1 domain [22] |
| ARHGAP5 | P190-B RhoGAP | 1.28 | RhoA, Rac1, [35] | FF, P-loop NTPase |
| SRGAP2 | | 1.10 | ND | FBAR, SH3 [36] |
| ARHGAP29 | PARG1 | 1.02 | RhoA | ZPH [37] |
| SLIT-ROBO | SRGAP3 | −1.13 | Rac, Cdc42 [38] | FBAR, SH3 |
| ARHGAP28 | | −1.34 | ND | Not reported |

ND, Not Determined.
*Modified from Table 1 in [6].
**Based on the NCBI database or literature.
doi:10.1371/journal.pone.0052258.t001

## β2-Chimaerin Localization at the Apical Membrane

The Chimaerin family is composed of two isoforms, α- and β-chimaerins. Each Chimaerin has two alternative splice variants, named α1 and α2-chimaerins, and β1 and β2-chimaerins, respectively. α2- and β2-chimaerins differ from α1 and β1-chimaerins in that the former contain an extended N-terminal region encompassing an SH2-type domain [19;20] (Figure 2E). α-chimaerin is also known as CHIMERIN 1 (Chn1), N-chimaerin, ARHGAP2, or RHOGAP2. β-chimaerin is also known as CHIMERIN 2 (Chn2), ARHGAP3, or RHOGAP3. All Chimaerins have a Rac-GAP domain and C1 domain [21]. In accordance with this structure, β2-chimaerin is recruited to the plasma membrane by the interaction of the C1 domain with DAG [22]. By the microarray analysis with dog cDNAs, we found that α1- and β2 chimaerin were expressed in MDCK cells to a detectable level. α2-chimarerin and β1-chimaerin have not been identified in the cDNA database of *Canis lupus familiaris* deposited in the NCBI database, nor with the microarray chip used in this study. We therefore called canine α1-chimaerin and β2-chimaerin Chn1 and Chn2, respectively, and investigated their roles further in this study.

To verify that Chimaerin is localized at the apical membrane, we established a MDCK cell line expressing GFP-tagged mouse Chn2 together with a cytosolic fluorescent red protein dKeima [23], and cultured the cells in Matrigel to form cysts. GFP-Chn2 localized mostly in the cytoplasm, but also accumulated at the apical membrane (Figure 2F, left panel). This plasma membrane accumulation of fluorescence was not observed for dKeima, which served as a control (middle panel). To confirm the plasma membrane accumulation of GFP-Chn2, a GFP/dKeima image was prepared in pseudocolor (Figure 2F, right panel), showing that GFP-Chn2 preferentially localized at the apical membrane. These results strongly suggest that Chimaerin(s) are recruited to the apical membrane by DAG binding, to inactivate Rac1. Our observation of uneven distribution of DAG during cystogenesis is consistent with the notion that upregulation of Chimaerin in the late stages is important for Rac1 inactivation in the mature cysts. Since there was no commercially-available antibody to detect the endogenous dog Chn1 or Chn2, we confirmed upregulation of Chn1 and Chn2 mRNAs by quantitative PCR (Figure 2G, and Fig. S3).

## Suppression of Rac1 Activation by Chimaerin

To examine whether Chn1 and Chn2 suppress Rac1 activation at the apical membrane, we depleted these proteins using a viral-mediated short hairpin RNA (shRNA) interference system. MDCK cells were infected with retroviruses containing shRNA sequences against Chn1 (shChn1), Chn2 (shChn2), or firefly Luciferase (shLuc) as a negative control [24]. The infected cells were selected with antibiotics. Knockdown efficiency was assessed by RT-PCR (Fig. S2). Knockdown MDCK cysts expressing Raichu-Rac1 were stimulated with HGF for 30 minutes or left unstimulated before acquisition of FRET ratio images. In control cysts, upon HGF treatment, Rac1 was activated weakly at the apical membrane (Figure 3A), but not at the lateral membrane (Figure 3B), suggesting that HGF stimulated GEF at the apical membrane. On the other hand, in shChn1 and shChn2 cysts, HGF treatment caused significant Rac1 activation at the apical membrane (Figure 3A), but not at the lateral membrane (Figure 3B). These data demonstrate that Chn1 and Chn2 suppress Rac1 activation upon HGF stimulation by inactivating Rac1 at the apical membrane.

We next examined the effect of knockdown of Chn1 and Chn2 in HGF-stimulated MDCK cysts. Two days after HGF treatment, cysts with luminal cell accumulation were counted. As shown in Figure 3C, 28% of cysts expressing shLuc RNA showed luminal cell accumulation. Knockdown of Chn1 and Chn2 significantly increased the percentage of abnormal cysts up to 59% and 49%, respectively. Similar results were obtained in cysts simultaneously depleted of both Chn1 and Chn2 (Fig. S4). The activation pattern of Rac1 as well as the morphology was visualized in these cysts (Figure 3D). The control cysts with shLuc expression showed a single lumen lined with monolayered cells (the upper row). A small number of cells were found in the lumen, but the FRET level was very low, indicating that these were dead cells (Figure 3D, the top panel). In the Chn1 knockdown or Chn2 knockdown cysts, a number of cells were accumulated in the cysts and formed a multiple layer of cells (Figure 3D, middle and bottom panels). In these multi-layered cells, Rac1 activity was uniform in the entire plasma membrane (red arrow head). Importantly, even in the Chn1 or Chn2-knockdown cysts, cells that maintained the monolayer structure exhibited lower Rac1 activity at the apical membrane than the lateral plasma membrane (white arrow head).

The results of the Chn1 and Chn2 knockdown experiments strongly suggest that Chn1 and Chn2 suppress Rac1 activity at the apical plasma membrane and that aberrant Rac1 activation at the apical membrane causes cells to lose their apico-basal polarity. Since conditional activation of Rac1 at the apical membrane causes luminal cell accumulation via tight junction breakdown, polarity loss, and misorientation of cell division, we speculate that Rac1 activation at the apical membrane caused by Chimaerin

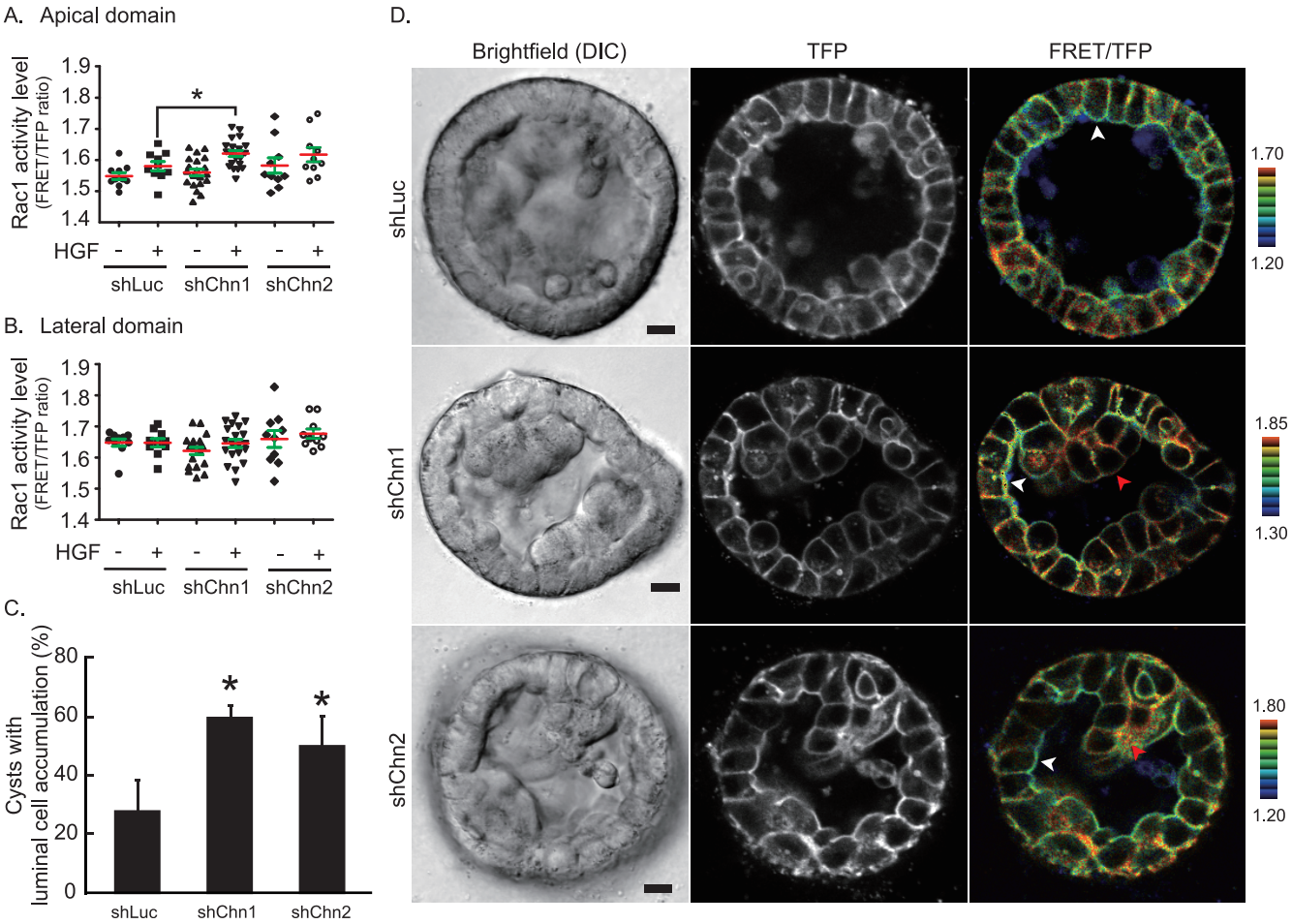


**Figure 3. Chn1 and Chn2 knockdown affect Rac1 activity and cyst morphology.** MDCK cyst expressing shLuc, shChn1, and shChn2 together with Raichu-Rac1 were stimulated with HGF for 30 minutes. And then Rac1 activity of the cells in the cyst wall was calculated at the apical membrane (A) and the lateral membrane (B). Red and green lines indicate the average of FRET/TFP ratios and SD, respectively. *$P<0.05$. (C) MDCK cysts expressing shLuc, shChn1, and shChn2 were treated with HGF for 2 days and imaged. Shown are the averages of three independent experiments with SD. The numbers of scored cysts are: Experiment (Exp.) 1 [n = 75 (shLuc), 62 (shChn1), 72 (shChn2)]; Exp2 [n = 80 (shLuc), 55 (shChn1), 66 (shChn2)]; Exp3 [60 (shLuc), 70 (shChn1), 61 (shChn2)]. *$P<0.05$. (D) Representative images of MDCK cysts expressing shLuc (upper), shChn1 (middle), and shChn2 (bottom) together with Raichu-Rac1. Bright-field images (left column), TFP images (middle column) were obtained with an inverted confocal microscope, and FRET/TFP ratio images (right column) were calculated. Bars indicate 10 μm. White arrowheads indicate low Rac1 activity at the apical domain. Red arrowheads indicate luminal cell accumulation showing high Rac1 activity through the whole plasma membrane.
doi:10.1371/journal.pone.0052258.g003

depletion utilizes the same pathways for the abnormal morphology [2]. We previously found that similar luminal cell filling was induced by the expression of constitutive active Ras protein in MDCK cysts [25]. For this, cell-cycle progression and anoikis prevention mediated by PI3 kinase were required. Since living cells were observed in the lumen in Chimaerin depleted cysts, it is possible that Chn1 and Chn2 participate in anoikis regulation.

## No Effect of Chn1 and Chn2 Depletion on HGF-induced Extension

Finally, to examine whether Chimaerin functions as the apical-specific GAP, Chimaerin-depleted cysts were treated with HGF, and the numbers of cysts with extensions were counted. As shown in Figure 4, HGF-induced extension was comparable among control (shLuc) and Chimaerin-depleted (Chn1 and Chn2) cysts. These data confirmed that Chimaerin-dependent Rac1 inactivation is limited to the apical membrane.

## Conclusions

Combining microarray analysis data and FRET images of lipid distribution, we found that Rac1-specific GAPs Chn1 and Chn2 are involved in the suppression of Rac1 activity at the apical plasma membrane of the mature cyst (Fig. 1C). GFP-tagged Chn2 was detected at the apical membrane (Fig. 2F), and depletion of Chn1 and Chn2 increased Rac1 activity at the apical membrane and luminal cell accumulation in HGF-stimulated cysts. These data collectively suggest that Chn1 and Chn2 suppress Rac1 at the plasma membrane to maintain the monolayer epithelium. Of note, we could dissect two intracellular events; the luminal cell filling at the apical membrane and extension of a tubular structure at the basal membrane. Since knockdown of Chn1 and Chn2 did not affect extension formation at the basal membrane (Fig. 4), and Rac1 is required for extension (Fig. 1B), searching for molecules or reagents that inhibit the Rac1-dependent extension may lead to a novel treatment for cancer invasion. Live imaging with FRET biosensors will facilitate such cell-based screening.

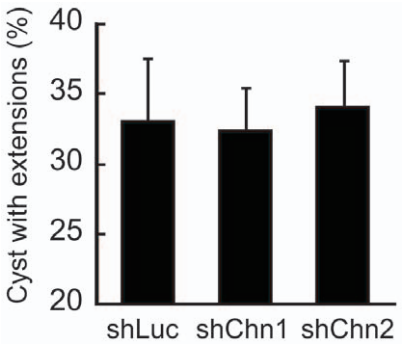


**Figure 4. Chn1 and Chn2 knockdown do not affect extension formation.** MDCK cysts expressing shLuc, shChn1, and shChn2 were treated with HGF for 12 hours. Cysts with at least one extension were counted. Shown are the averages of three independent experiments with SD. The numbers of scored cysts are: Experiment (Exp.) 1 [n = 34 (shLuc), 36 (shChn1), 38 (shChn2)]; Exp2 [n = 28 (shLuc), 30 (shChn1), 32 (shChn2)]; Exp3 [37 (shLuc), 31 (shChn1), 32 (shChn2)].
doi:10.1371/journal.pone.0052258.g004

α1-chimaerin cDNA was originally isolated from brain, and its distribution is restricted to brain and testis [19]. α2-chimearin is also expressed in the brain, and in other organs such as heart, intestine, and lung to a lesser extent [26]. Mice carrying spontaneous mutations in α1 and α2-chimaerin showed a rabbit-like hopping gait, impaired corticospinal axon guidance, and abnormal spinal central pattern generators [27]. β1-chimaerin was originally identified as a testis-specific RacGAP [28]. Using an antibody against β1-chimaerin, the β2-chimaerin isoform was discovered in the brain [29]. β2-chimaerin knockout mice were generated to show that β2-chimaerin is required for presynaptic pruning in the hippocampus [30]. Although the role of Chimaerins in the epithelial structure has not been fully investigated, it has been suggested that β2-chimaerin controls progression of malignant glioma, based on the fact that β2-chimaerin is down-regulated in high-grade glioma [31]. It has also been reported that β2-chimaerin expression was reduced in breast cancer cell lines and tumors [31]. In MDCK cells, both Chn1 and Chn2 are required to maintain the cyst structure (Fig. 3). Although we could not compare protein levels of Chn1 and Chn2, it is speculated that both are equally expressed in MDCK cells, because either Chn1 or Chn2 depletion caused Rac1 activation and luminal cell accumulation. Moreover, it is speculated that the SH2 domain in Chn2 is not required to maintain the cyst structure (Fig. 2E). Since we believe that luminal cell accumulation corresponds to benign hyperplasia in the body, additional mutations or expression changes of other genes will be required for progression. Further clinical surveys of benign and malignant tumors will determine whether Chimaerin can be a target for therapy.

## Supporting Information

**Figure S1 Schematic representation of a rapamycin-inducible Rac1 activity manipulation system (Corresponding to Figure 1B).** In this system, rapamycin induces the hetero-dimerization of FK506-binding protein (FKBP)-fused proteins and FKBP12-rapamycin binding domain (FRB)-fused proteins. In cells expressing Lyn-FRB, an FRB protein anchored at the plasma membrane, the FKBP-fused GAP domain translocates from the cytosol to the plasma membrane upon rapamycin treatment.
(EPS)

**Figure S2 Schematic representation of a monitor for Diacylglycerol (DAG) (Corresponding to Figure 2)**. YFP and TFP denote a yellow-emitting mutant of GFP and teal fluorescent protein, respectively. K-Ras4B-CT (blue box) and Gly-Gly indicates the C-terminal region of K-Ras4B and glycine-glycine linker, respectively. The C1 domain of PKCβII was utilized as the DAG-binding domain. In this biosensor design, the FRET level will increase when the biosensor recognizes DAG (right)
(EPS)

**Figure S3 Quantification of Chimaerin Knockdown (Corresponding to Figure 3).** Total RNA was extracted from MDCK cells expressing shLuc, shChn1, and shChn2. After reverse transcription, relative mRNA levels of Chn1 (A) and Chn2 (B) over control shLuc were quantified. Shown are the averages of three independent experiments with SD (n = 3).
(EPS)

**Figure S4** Combined Chn1 and Chn2 knockdown affects cyst morphology (Corresponding to Figure 3C). MDCK cysts expressing both shChn1 and shChn2 together were treated with HGF for 2 days and imaged. Shown are the averages of three independent experiments with SD. The numbers of scored cysts are: Experiment (Exp.) 1 [n = 72 (−HGF), 99 (+HGF)]; Exp2 [n = 61 (−HGF), 87 (+HGF)]; Exp3 [n = 76 (−HGF), 67 (+HGF)]. *P<0.05.
(EPS)

**Table S1 List of GAPs for Rho family GTPases in the microarray analysis.** Genes whose mRNA is upregulated in the late stages (magenta) or downregulated (blue). Genes whose mRNA levels were not certified were labeled with gray.
(EPS)

## Acknowledgments

We are grateful to Drs. Hironori Katoh (Kyoto University) for the generous gift of the β2-chimaerin plasmid. We also are grateful to Mss. Y. Inaoka, K. Hirano, A. Kawagishi, K. Miyamoto, and N. Nonaka for their technical assistance, and Dr. James Hejna and the staff at the Matsuda laboratory for their technical advice and helpful input.

## Author Contributions

Conceived and designed the experiments: SY MM EK. Performed the experiments: SY. Analyzed the data: SY EK. Contributed reagents/materials/analysis tools: SY MM EK. Wrote the paper: SY MM EK.

## References

1. O'Brien LE, Zegers MM, Mostov KE (2002) Opinion: Building epithelial architecture: insights from three-dimensional culture models. Nat Rev Mol Cell Biol 3: 531–537.
2. Yagi S, Matsuda M, Kiyokawa E (2012) Suppression of Rac1 activity at the apical membrane of MDCK cells is essential for cyst structure maintenance. EMBO Rep 13: 237–243.
3. Kiyokawa E, Aoki K, Nakamura T, Matsuda M (2010) Spatiotemporal regulation of small GTPases as revealed by probes based on the principle of Förster Resonance Energy Transfer (FRET): Implications for signaling and pharmacology. Annu Rev Pharmacol Toxicol 51: 337–358.
4. Rossman KL, Der CJ, Sondek J (2005) GEF means go: turning on RHO GTPases with guanine nucleotide-exchange factors. Nat Rev Mol Cell Biol 6: 167–180.
5. Vigil D, Cherfils J, Rossman KL, Der CJ (2010) Ras superfamily GEFs and GAPs: validated and tractable targets for cancer therapy? Nat Rev Cancer 10: 842–857.

6. Tcherkezian J, Lamarche-Vane N (2007) Current knowledge of the large RhoGAP family of proteins. Biol Cell 99: 67–86.
7. Schmidt A, Hall A (2002) Guanine nucleotide exchange factors for Rho GTPases: turning on the switch. Genes Dev 16: 1587–1609.
8. Rodriguez-Fraticelli AE, Vergarajauregui S, Eastburn DJ, Datta A, Alonso MA, et al. (2010) The Cdc42 GEF Intersectin 2 controls mitotic spindle orientation to form the lumen during epithelial morphogenesis. J Cell Biol 189: 725–738.
9. Qin Y, Meisen WH, Hao Y, Macara IG (2010) Tuba, a Cdc42 GEF, is required for polarized spindle orientation during epithelial cyst formation. J Cell Biol 189: 661–669.
10. Itoh RE, Kurokawa K, Ohba Y, Yoshizaki H, Mochizuki N, et al. (2002) Activation of rac and cdc42 video imaged by fluorescent resonance energy transfer-based single-molecule probes in the membrane of living cells. Mol Cell Biol 22: 6582–6591.
11. Nishioka T, Aoki K, Hikake K, Yoshizaki H, Kiyokawa E, et al. (2008) Rapid Turnover Rate of Phosphoinositides at the Front of Migrating MDCK Cells. Mol Biol Cell 19: 4213–4223.
12. Aoki K, Nakamura T, Inoue T, Meyer T, Matsuda M (2007) An essential role for the SHIP2-dependent negative feedback loop in neuritogenesis of nerve growth factor-stimulated PC12 cells. J Cell Biol 177: 817–827.
13. Montesano R, Matsumoto K, Nakamura T, Orci L (1991) Identification of a fibroblast-derived epithelial morphogen as hepatocyte growth factor. Cell 67: 901–908.
14. Yoshizaki H, Mochizuki N, Gotoh Y, Matsuda M (2007) Akt-PDK1 Complex Mediates Epidermal Growth Factor-induced Membrane Protrusion through Ral Activation. Mol Biol Cell 18: 119–128.
15. Aoki K, Nakamura T, Fujikawa K, Matsuda M (2005) Local Phosphatidylinositol 3,4,5-Trisphosphate Accumulation Recruits Vav2 and Vav3 to Activate Rac1/Cdc42 and Initiate Neurite Outgrowth in Nerve Growth Factor-stimulated PC12 Cells. Mol Biol Cell 16: 2207–2217.
16. Kumagai Y, Kamioka Y, Yagi S, Matsuda M, Kiyokawa E (2011) A genetically encoded Forster resonance energy transfer biosensor for two-photon excitation microscopy. Anal Biochem 413: 192–199.
17. Martin-Belmonte F, Gassama A, Datta A, Yu W, Rescher U, Gerke V, et al. (2007) PTEN-Mediated Apical Segregation of Phosphoinositides Controls Epithelial Morphogenesis through Cdc42. Cell 128: 383–397.
18. Farmer P, Bonnefoi H, Anderle P, Cameron D, Wirapati P, et al. (2009) A stroma-related gene signature predicts resistance to neoadjuvant chemotherapy in breast cancer. Nat Med 15: 68–74.
19. Hall C, Monfries C, Smith P, Lim HH, Kozma R, et al. (1990) Novel human brain cDNA encoding a 34,000 Mr protein n-chimaerin, related to both the regulatory domain of protein kinase C and BCR, the product of the breakpoint cluster region gene. J Mol Biol 211: 11–16.
20. Hall C, Michael GJ, Cann N, Ferrari G, Teo M, et al. (2001) alpha2-chimaerin, a Cdc42/Rac1 regulator, is selectively expressed in the rat embryonic nervous system and is involved in neuritogenesis in N1E-115 neuroblastoma cells. J Neurosci 21: 5191–5202.
21. Yang C, Kazanietz MG (2007) Chimaerins: GAPs that bridge diacylglycerol signalling and the small G-protein Rac. Biochem J 403: 1–12.
22. Caloca MJ, Garcia-Bermejo ML, Blumberg PM, Lewin NE, Kremmer E, et al. (1999) beta2-chimaerin is a novel target for diacylglycerol: binding properties and changes in subcellular localization mediated by ligand binding to its C1 domain. Proc Natl Acad Sci U S A 96: 11854–11859.
23. Kogure T, Karasawa S, Araki T, Saito K, Kinjo M, et al.(2006) A fluorescent variant of a protein from the stony coral Montipora facilitates dual-color single-laser fluorescence cross-correlation spectroscopy. Nat Biotech 24: 577–581.
24. Hara S, Kiyokawa E, Iemura S, Natsume T, Wassmer T, et al. (2008) The DHR1 domain of DOCK180 binds to SNX5 and regulates cation-independent mannose 6-phosphate receptor transport. Mol Biol Cell 19: 3823–3835.
25. Sakurai A, Matsuda M, Kiyokawa E (2012) Activated Ras protein accelerates cell cycle progression to perturb MDCK cystogenesis. J Biol Chem 287: 31703–31711.
26. Hall C, Sin WC, Teo M, Michael GJ, Smith P, et al. (1993) Alpha 2-chimerin, an SH2-containing GTPase-activating protein for the ras-related protein p21rac derived by alternate splicing of the human n-chimerin gene, is selectively expressed in brain regions and testes. Mol Cell Biol 13: 4986–4998.
27. Iwasato T, Katoh H, Nishimaru H, Ishikawa Y, Inoue H, et al. (2007) Rac-GAP alpha-chimerin regulates motor-circuit formation as a key mediator of EphrinB3/EphA4 forward signaling. Cell 130: 742–753.
28. Leung T, How BE, Manser E, Lim L (1993) Germ cell beta-chimaerin, a new GTPase-activating protein for p21rac, is specifically expressed during the acrosomal assembly stage in rat testis. J Biol Chem 268: 3813–3816.
29. Leung T, How BE, Manser E, Lim L (1994) Cerebellar beta 2-chimaerin, a GTPase-activating protein for p21 ras-related rac is specifically expressed in granule cells and has a unique N-terminal SH2 domain. J Biol Chem 269: 12888–12892.
30. Riccomagno MM, Hurtado A, Wang H, Macopson JG, Griner EM, et al. (2012) The RacGAP β2-Chimaerin Selectively Mediates Axonal Pruning in the Hippocampus. Cell 149: 1594–1606.
31. Yang C, Liu Y, Leskow FC, Weaver VM, Kazanietz MG (2005) Rac-GAP-dependent inhibition of breast cancer cell proliferation by β2-chimerin. J Biol Chem 280: 24363–24370.
32. Ohta Y, Hartwig JH, Stossel TP (2006) FilGAP, a Rho- and ROCK-regulated GAP for Rac binds filamin A to control actin remodelling. Nat Cell Biol 8: 803–814.
33. Kozma R, Ahmed S, Best A, Lim L (1996) The GTPase-activating protein n-chimaerin cooperates with Rac1 and Cdc42Hs to induce the formation of lamellipodia and filopodia. Mol Cell Biol 16: 5069–5080.
34. Caloca MJ, Wang H, Kazanietz MG (2003) Characterization of the Rac-GAP (Rac-GTPase-activating protein) activity of beta2-chimaerin, a 'non-protein kinase C' phorbol ester receptor. Biochem J 375: 313–321.
35. Burbelo PD, Miyamoto S, Utani A, Brill S, Yamada KM, et al. (1995) p190-B, a New Member of the Rho GAP Family, and Rho Are Induced to Cluster after Integrin Cross-linking. J Biol Chem 270: 30919–30926.
36. Charrier C, Joshi K, Coutinho-Budd J, Kim JE, Lambert N, et al. (2012) Inhibition of SRGAP2 Function by Its Human-Specific Paralogs Induces Neoteny during Spine Maturation. Cell 149: 923–935.
37. Saras J, Franzen P, Aspenstrom P, Hellman U, Gonez LJ, et al. (1997) A Novel GTPase-activating Protein for Rho Interacts with a PDZ Domain of the Protein-tyrosine Phosphatase PTPL1. J Biol Chem 272: 24333–24338.
38. Wong K, Ren XR, Huang YZ, Xie Y, Liu G, et al. (2001) Signal Transduction in Neuronal Migration: Roles of GTPase Activating Proteins and the Small GTPase Cdc42 in the Slit-Robo Pathway. Cell 107: 209–221.